

Arcing Fault Detection with Experimental Verification using Antenna for Signal Capture of Radiated Electromagnetic Energy

Charles Kim¹ and Robert Sowah
Washington, DC 20059

Abstract

Arcing faults are prevalent in modern terrestrial, space and naval power systems. They are responsible for the most devastating effects in such systems as they tend to be soft faults waiting to wreak havoc on pertinent system components. Recent mishaps and tragic accidents due to arcing faults brought renewed attention to this vexing problem and, since then, there has been much research effort to early-detect incipient electrical wiring faults using their pertinent signatures. It is important that incipient arcing faults within any mission-critical systems be detected, located, and isolated within a system before causing major problems. The novel approach presented in the paper is the use of two types of antennas to sense the electromagnetic energy radiated from arcing. Based on the staged arcing faults and the consequent recording of the faulted scenarios using loop and stick antennas, the merits of detection of arc from electrical wire and switch are evaluated. Detailed antenna construction, experimental set-up and results for sensitive but discriminative detection are discussed for incorporation of the overall system design into realistic implementation.

I. Arcing Faults

Mission-critical systems operated by the navy, air force and aerospace industries recognized that electrical fires were becoming a major problem in submarines and aircrafts such as fighter jets during missions. About three fires per year were occurring in the main electrical distribution switchboards across the submarine fleet of the US Navy¹. Those fires have had a major impact on mission-readiness and could potentially cause loss of life, ship and aircraft (e.g. the loss of lives when TWA aircraft went down due to arc igniting the fuel system). In three-quarters of a second, the current from the smallest generator can burn a fist-sized hole in the side of a switchboard. The damage initially increases exponentially with time, limited only by available current from the generators².

The ship electrical power system is made up of propulsion loads, ship service loads, which comprises of combat system loads and auxiliary ship service loads such as the power conversion equipment, the A/C Heating systems, hotels, shops and other miscellaneous Electronic loads. This combination of system loads and its compactness increases its complexity and vulnerability to arcing fault hazards. An arcing fault is a dangerous form of short-circuit that may have a low current magnitude³. An arc of several hundred amps can exist and not cause a breaker to open, since normal loads draw much more current. An arc is not a short circuit but a resistive load yielding heat; therefore, the breakers do not open. Faulty connections due to corrosion, faulty initial fastening, vibration, etc., cause 60-80% of arcs¹.

The magnitude of an arc fault current is limited by the resistance of the arc and the impedance of the ground return path. This low level of fault current is often insufficient to immediately trip overcurrent devices installed within the vicinity of the arc fault, resulting in the escalation of the arcing fault, increased system damage, tremendous release of energy and threat to human life. On the other hand, high impedance faults (HIF) result when an energized primary conductor comes in contact with a quasi-insulating object such as an equipment or ground. It is characterized by sufficiently high impedance. It produces current levels in the order of 0 to 50 ampere range. An arc fault is a high power discharge of electricity between two or more conductors. Arcs may be initiated in three ways: through spark discharge, physical contact, and glow-to-arc transition. Figure 1 shows extensive damage caused by a typical electrical fire initiated by an arc within mission-critical systems in a navy ship.

¹ Charles Kim is a professor in the Department of Electrical and Computer Engineering at Howard University. 2300 Sixth St. NW, Washington DC 20059. Robert Sowah is a graduate student.



Figure 1: Damage from an arc-generated electrical fire (USS Parche (SSN 683))¹

On the other hand, an evaluation of a ten-year period showed 271 Air Force aircraft mishaps that were directly related to the electrical power system problems. Among those contributing components, the generating constituent had a large share with 18% of all electrical power system faults. Conductors led with 29% of all electrically related mishaps. Batteries caused about 1% of the mishaps, while transformers share about 6% of the caused problems⁴. In all, electrical faults exemplified by arcing and spark contribute major mishaps in aircraft. Early detection and location of such faults would save lives and maintenance costs.

This paper first introduces the background of arcing faults, their destructive capabilities and the need for adequate detection since they evade the settings of the protection system devices of a typical power system. Next, we discuss about the mathematical modeling of arcing faults including an electromagnetic radiation model that we utilized in the research. Then, section 3 presents the experimental set up for the arcing fault signal captures using antennae of the radiated electromagnetic energy generated from arc. In section 4 we presents the results of the experiments. Lastly, we outline the main conclusions based on the experiments and, as future works, application benefits this approach offers to arcing fault detection and location.

II. Arcing Fault Models

One major characteristic of arcing fault currents is that they are discontinuous, nonlinear and non-sinusoidal and are limited by the ground return path impedance and the arc voltage. This discontinuity and nonlinearity is most prominent in arcing fault modeling in order to mimic the real arc faults. There are various models developed by various researchers that are worthy of mention.

Kaufmann and Page employed an instantaneous arc current model: this model stipulates that an arc current begins to flow when the supply voltage provides the necessary re-strike potential⁵. The arc current flows continuously until the stored magnetic energy associated with the system's inductance had been dissipated. The arc current remains zero, until the magnitude of the supply voltage equals the re-strike voltage; at this point, the arc re-strikes with the opposite polarity.

Protective devices are usually not very sensitive to parallel arcing fault since their current magnitude are less than that of normal operating current of the system being protected. There are two major approaches to arcing fault model representation: arcing fault model for conventional power systems and arcing fault model for circuit breaker interruption of naval and aerospace systems. In addition to the traditional arcing model of arc current or arc voltage, we introduce an electromagnetic radiation model on which our experiment is primarily based on.

A. Conventional power systems arcing fault model

Several models of arc fault modeling equations have evolved over time for representing behavior of arcing fault in power system operation. However, the instantaneous arcing fault current model better presents the failure physics of the arc. The instantaneous arc current model, relying on inductive circuit, is based on energy balance and incorporates a flat-topped arc voltage^{3, 5-6}. The arc current in the model is described by,

$$i_{arc} = \int_{t \Rightarrow t_a}^t (V_{max} \cos \omega t - V_{arc}) dt \quad \text{where } t_a = \frac{1}{\omega} \arcsin \left(\frac{V_{restrike}}{V_{max}} \right).$$

As a variant of the instantaneous arc current model, a differential equation based arcing fault model can be easily derived as follows:

$$V_{max} \cos \omega t = i_{arc} R + L \frac{di_{arc}}{dt} + V_{arc}$$

Then, a variant of the classic differential equation model is given below following series of experiments conducted by the researchers⁵.

$$V_{max} \sin \omega t = i_{arc} R + L \frac{di_{arc}}{dt} + (20 + 534g)t_{arc}^k$$

where g is arc conductance, and the constant k is related to luminance of the arc which is in the range of $0.12 \leq k \leq 0.5$ depending on the arcing medium, the voltage and current levels at which the arc occurs. These equations above are based on free-air arcs generated between both copper and aluminum electrodes of about 1.2 cm^{5,7}.

B. Arc Models for Circuit Breaker Interruption of Naval and Space systems

Different types of arc modeling for circuit breaker interruption have evolved over the years for mimicking the behavior of arc in electrical installations for both naval and space systems. The primary models are Mayr and Cassie models which relate arc conductance with arc voltage and arc time^{3,8}. Two models are almost identical except that one relates arc conductance with arc voltage over arc power, and the other arc conductance with arc voltage over fixed arc voltage. Both types of arc representation have a common property that the arc current depends largely on the magnitude of the line impedance (the X/R ratio) and the arc gap length. The mathematical models of Cassie and Mayr arc shown in the following two equations:

$$\text{Mayr arc model : } \frac{1}{g} \frac{dg}{dt} = \frac{d \ln g}{dt} = \frac{1}{\tau} \left(\frac{ui}{P} - 1 \right),$$

$$\text{Cassie arc model: } \frac{1}{g} \frac{dg}{dt} = \frac{d \ln g}{dt} = \frac{1}{\tau} \left(\frac{u^2}{U_c^2} - 1 \right),$$

where g : arc conductance

u : arc voltage

i : arc current

τ : arc time constant

P : cooling power of arc (arc loss constant)

U_c : constant arc voltage

C. Electromagnetic Energy Radiation Model

Basically the above two models describe arcing faults in terms of voltages and currents. Our model for detection of arcing faults relies on the electromagnetic energy radiated from an arcing source, since arcing faults are accompanied by radiation in the form of heat, sound and electromagnetic waves⁹.

Rompe and Weisel conductivity law in physics provides the temporal evolution of the conductivity during the electronic multiplication process. This conductivity law associated with a propagation equation given the electric field value of each point of the transient arc zone leads to the space-time evolution of current and potential

(voltage)¹⁰. The calculation of the current variation thus leads to the determination of intensity and spectral content of the radiated electric field associated with the transient arc.

Mathematically put, the general expression for the electromagnetic field E_{rad} radiated at a distance R by a current component of length δ oriented along the x-axis is given as:

$$E_{rad}(R,t) = \frac{\sin\theta}{4\pi\epsilon_0 Rc^2} \int_0^\delta \frac{di}{dt} dx$$

where θ is the angle between current direction and the R vector and c is the velocity of light. The complete variation of current on the element of length δ can be written in the discharge form as:

$$\frac{di}{dt} = \frac{\delta i}{\delta t} + \frac{\delta i}{\delta x} \frac{dx}{dt}$$

During the formation of the transient arc, the deformation of the initial potential pattern leads to partial variation of $\frac{\delta i}{\delta t}$ in the discharge frames.

Under steady state propagation conditions the radiated electric field E_{rad} becomes:

$$E_{rad}(R,t) = \frac{\sin\theta}{4\pi\epsilon_0 Rc^2} \int_0^\delta \frac{\delta i}{\delta x} \frac{\delta x}{\delta t} dx, \quad \text{which reduces to } E_{rad}(R,t) = \frac{\sin\theta}{4\pi\epsilon_0 Rc^2} v \Delta i$$

where v is the steady state propagation speed of the discharge and $\Delta i = i_{\max} - i_o$, where i_o is the current associated with the primary breakdown phase before the development of the transient arc and i_{\max} is the peak current at the beginning of the propagation.

The discharge and the short gap breakdowns at atmospheric pressure shows a current phase characterized by a fast rising front. There are two phases: the transient arc phase which takes place in the breakdown mechanisms and the development of the conductive channel between the electrodes¹⁰. This strong ionization phase lasting from 5 to 10 ns may be the source of the VHF and UHF radiation emitted during the different phases of natural lightning and the conducted arcing experiments.

III. Experimental Setup for Staged Arcing Faults and Radiated Signal Capturing

A. Detection of Radiated Electromagnetic Energy from Arc

Electromagnetic radiation can be detected using antenna. Antenna receives broad spectrum of frequencies when arc is initiated during the experiments. The spectral content of the radiated electromagnetic energy, even though the study in Ref. 10 did not explicitly experimented, is composed of low and high frequency components generated in the phases of the transient arc and conductive channel. If we design two antennas for low and high frequency capture of the arc, we can provide more certainty in the detection of arc. Moreover, the combination of antennas for both bands of frequency, high and low, can be further justified by the fact that the detection of both frequency components provides discrimination against normal radiation sources.

A detection scheme of the research is that the electromagnetic radiation energy is picked up by stick and loop antennas. Both antennas are susceptible to different frequency ranges and therefore offer different discriminatory analysis of the staged arcing fault experiments. Basically, the two antennas had different sensitivities for different frequency ranges of the radiated electromagnetic waves from the arcing source based on their construction and depending upon initial pre-fault conditions and post fault conditions.

B. Experimental Set-up

The experimental set up is depicted in the Figure 2 below with its associated measurement tools. Signals

were measured from a staged arcing fault between two electrodes. Different measurement resolution rates were utilized for the signal capture. Initially, the only load present was the masking load. Then the switch was closed to apply a current limited carbonized fault. By applying current to the carbon electrodes and varying the gap lengths, arcing faults are initiated with varying spectral content. This can be seen on the data trace as an increase in current with a rather ragged appearance on the current envelope. The signal measurement system incorporates loop and stick antennae for arcing fault signal capture and transmission for eventual processing of the signatures.

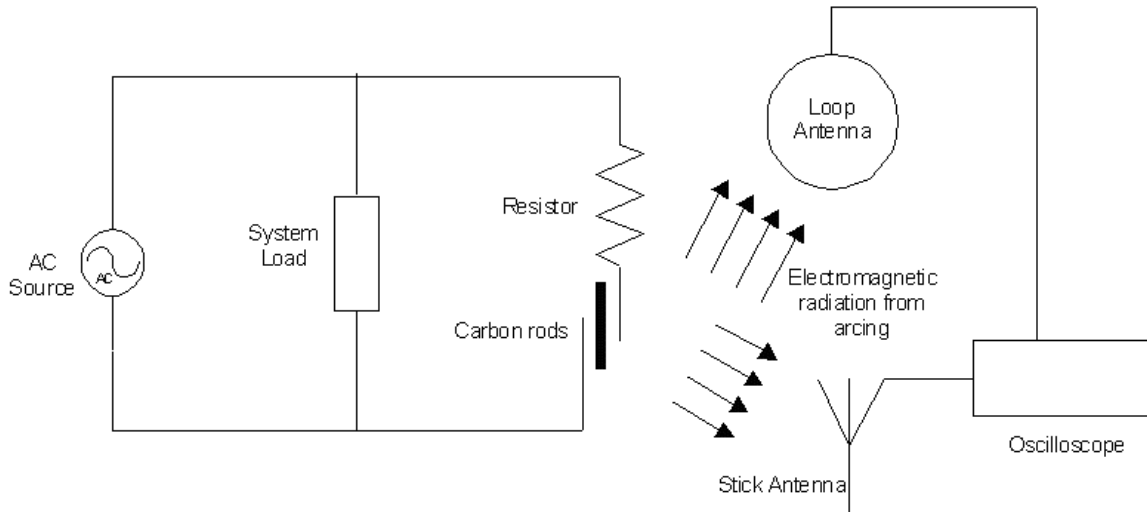


Figure 2: Schematic diagram of the experimental set up characterization of arcing faults using loop and stick antennae

1. Loop antenna

A loop antenna is primarily suited for the AM broadcast and long wave bands. There are two different types of loop antennas namely: ferrite bar loop antenna and air core loop antenna. A loop antenna is directional with a figure eight pickup pattern. The loop allows signals on opposite sides to be received, while off the sides of the loop, the signal decrease or cancels out. This nullifying feature allows the removal of a local station on a frequency and pick up another on the same frequency by removing the local signal. Air core loop antennas vary in sizes and tend to proportionally gain signal strength with loop size. A small loop encounters signal loss hence the need for signal amplification before processing.

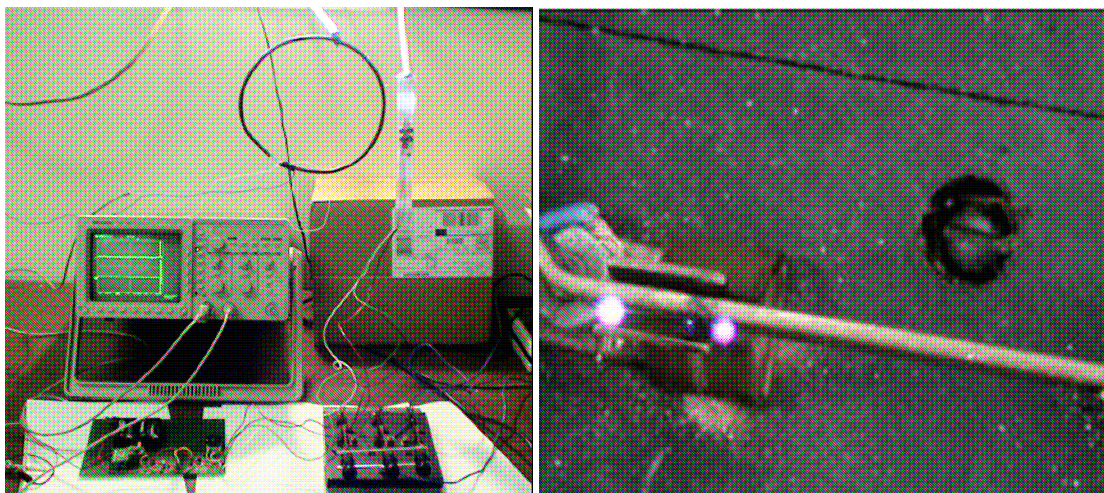


Figure 3: Actual photographs of the experimental set ups for signal capture using the loop and stick antennas for data processing. Also shown, at right, is arc/spark generated from the knife switch.

The number of turns of the loop is determined by the overall size of the antenna, its frequency range and the tuning capacitor and how tightly the wires are packaged together. The larger the loop the fewer the turns required. The optimum number of turns for maximum range is also affected by the close proximity of metal. Metals with having different magnetic permeability will exhibit different achievable ranges. The air-core loop antenna we used in the experiment is designed to tune in to about 100MHz frequency band.

2. Stick Antenna

A ferrite rod is used to increase magnetic flux density without appreciable energy losses at the transmission frequency. The concentrated flux lines at the ends of the ferrite rod focus the field pattern. This effect tends to increase the transmission distance while in the main lobe of the beam whereas the field outside decays rapidly with distance. The stick antenna of ferrite rod used in the experiment is utilized from an AM/FM antenna.

IV. Testing and Experimental Results

During the arc discharge, electric currents are induced by moving charges. These charges are conveyed by time-varying electric fields according to Maxwell's equations; they are equivalent to current pulses which give rise to the time-varying electromagnetic interference field or radio noise or radio interference as referenced in published literature. These variations being nonlinear and time-varying spikes are picked up by the antennas utilized, hence the display on the scope thus giving the random nature of the electromagnetic radiation. This characteristic feature enables detection of arc faults to be verified experimentally.

A. Stick antenna test

These figures depict the current record acquired for a few cycles before and after the arc initiation. A single channel was utilized in capturing signals from the stick antenna. In Figure 4 are two shots of the same waveform in different time/div, which offer details of the captured signal characteristics in terms of frequency, and the detection performance of the stick antennas, under varying frequency ranges and sampling rates.

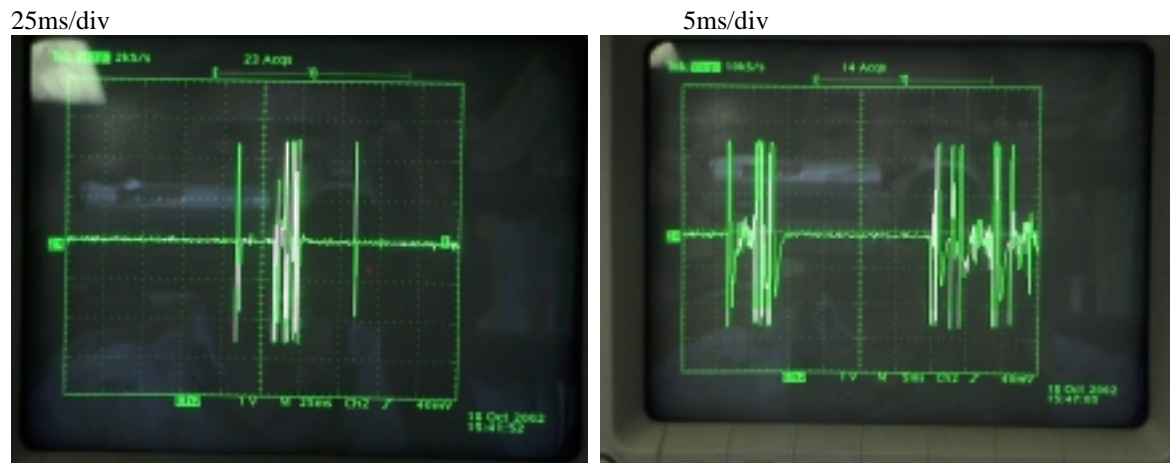


Figure 4: Actual photoshots of the captured signal by the stick antenna in different time/divisions.

B. Loop antenna test

The staged arcing fault signature captured using the loop antenna is displayed on the oscilloscope in Figure 5. The loop antenna with its greater field of data capture acquires more of the faulted signatures (electromagnetic radiation) of high frequency within the VHF and UHF bands than that compared to the stick antenna.

2.5 μ s/div



Figure 5: Actual photoshot of teh captured signal from the loop antenna.

C. Loop and stick antenna test

Two channels were utilized for data capture of the faulted signal from the two antennas (both loop and stick) simulataneously. In Figure 6 are two different shots of the same waveform in different time/div, which tell (1) the captured signal characteristics in terms of frequency, and (2) the detection performance of two different antennas thereby offering offering insight into the suitability of each antenna for specific frequency ranges and sampling rates. It offers a form of discrimination of normal system events viz-a-viz faulted scenarios.

1ms/div



1 μ s/div

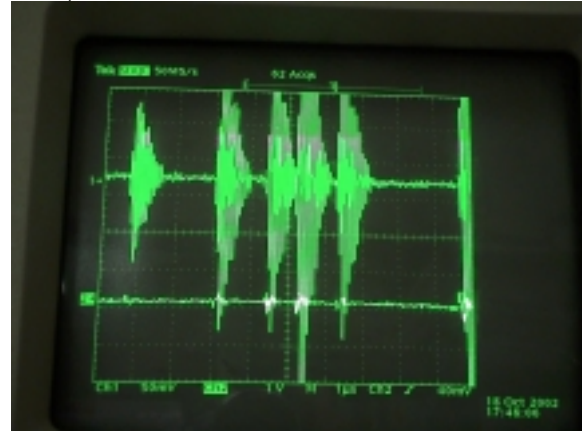


Figure 6: Actual photoshots of the captured signals by the stick and loop antennas. Top tracings are from loop antenna and, the bottom ones, from stick antenna.

The first channel (top tracing) represents data capture by the loop antenna while the second channel (bottom tracing) represents data capture by the stick antenna. Based on the conducted experiments, the two antennas utilized offer efficient discrimination as they capture very salient features of the ensuing arc under different frequencies and sampling rates. The loop antenna is less sensitive to low frequency electromagnetic radiation signal from the staged arc fault where as the stick antenna does. However, electromagnetic radiations of high frequency within the VHF and UHF bands are easily detected by the loop antenna whilst the stick antenna is not responsive enough.

V. Conclusions and Future Work

The novel approach presented involved the use of two types of antennas simultaneously to sense the electromagnetic energy radiated from the arcing faults. Based on the staged arcing faults, loop and stick antennas acquired faulted data and transmitted to the oscilloscope for visualization with different frequency ranges. The merits of detection of arc based on its electromagnetic radiation from two electrodes are evaluated. Basically, the wide field of view of the loop antenna favors more data capture within the VHF and UHF bands and enables ease of processing and visualization of arcs within those frequency bands compared to the stick antenna which offer some limited information of a fault within the same band. Moreover, the combination of the two antennas offers greater discrimination of faults from normal system events with enhanced pertinent data for ease of processing and visualization.

The collected data from sensors will enable parametric analysis to pseudo-optimize the detection capability while maintaining a high degree of insensitivity to normal system events. Based on the overall design and hardware with its associated modularity, it can be incorporated into an instrumentation device as a realistic implementation of onboard naval and aircraft power systems for arcing faults detection.

Location of arcing faults within the system wide environment using the electromagnetic energy radiation and the reconfiguration and/or restoration of system components has been of interest to the researchers and will form a major part of our future research efforts.

VI. References

- [1] H. Bruce Land III, Christopher L. Eddins, and John M. Klimek. "Evolution of Arc Fault Protection Technology at APL", Technical Report. <http://techdigest.jhuapl.edu/td2502/Land.pdf>
- [2] P. Meckler, K.J. Eichhorn and W. Ho, "Detecting and extinguishing of arcs in aircraft electrical systems", *Proc. 2001 Aerospace Congress*, SAE-2001-01-2657, Sept. 10-14, 2001.
- [3] T. Gammon and J. Matthews, "The historical evolution of arcing-fault models for low-voltage systems," in *Conf. Rec. 1999 IEEE I&CPS Tech. Conf.*, Sparks, NV, May 1999, pp. 1–6.
- [4] Slenski, G. A., Walz, M. F., "Novel Technologies for Improving Wire System Integrity," *Ninth Aging Aircraft Conference*, Atlanta, March 6-9, 2006
- [5] R. H. Kaufmann and J. C. Page, "Arcing fault protection for low-voltage power distribution systems—Nature of the problem," *AIEE Trans.*, pp. 160–167, June 1960.
- [6] U. Habedank: "Application of a New Arc Model for the Evaluation of Short-Circuit Breaking Tests". *IEEE Trans. Power Delivery*, vol. 8, no. 4, pp. 1921-1925, October 1993.
- [7] J. R. Dunki-Jacobs, "The effects of arcing ground faults on low-voltage system design," *IEEE Trans. Industry Applications*, vol. IA-8, pp. 223–230, May/June 1972.
- [8] P. H. Schavemaker, L. van der Sluis: "An Improved Mayr-Type Arc Model Based on Current-Zero Measurements". *IEEE Trans. Power Delivery*, vol. 15, no. 2, pp. 580-584, April 2000.
- [9] T.S. Sidhu, Gurdeep Singh and M.S. Sachdev, "Microprocessor based Instrument for Detecting and locating Electric Arcs" *IEEE Transactions on Power Delivery*, Vol. 13, No. 4, October 1998.
- [10] A. Bondiou, G. Labaune, and J.P. Marque "Electromagnetic radiation associated with the formation of an electric arc breakdown in air at atmospheric pressure," *Journal of Applied Physics*, 61(2), January 1987.